UDC 537.874; 621.373

V.V. Grimalsky, Ph.D., S.V. Koshevaya, Dr. Sci., J. Escobedo-A., Ph.D.
(CIICAp, IICBA, Autonomous University of State Morelos, Cuernavaca, Mexico)
Yu.G. Rapoport, Dr. Sci.
(*Physical Fac., Taras Shevchenko National University of Kyiv, Kyiv, Ukraine)*

Formation of ultrashort pulses of THz range in narrow- gap semiconductors

The nonlinear propagation of transversely bounded terahertz pulses in bulk narrow-gap semiconductors like n-InSb is investigated theoretically. The cubic nonlinearity is due to the nonstandard dependence of the electron energy on the quasi-momentum. The nonlinearity possesses the focusing character both in longitudinal and transverse directions. The direct simulations are realized by FDTD method. The extreme narrowing of terahertz pulses occurs. The role of nonlinear dissipation is discussed.

Introduction.

The electromagnetic (EM) radiation of the terahertz (THz) range f = 100 GHz - 30 THz is used in spectroscopy, medicine, introscopy, and environmental science [1,2]. In THz range under the temperatures $T \geq 77$ K narrow-gap semiconductors like InSb, InAs, $Cd_xHg_{1-x}Te$ possess the nonlinearity due to the nonparabolicity of the electron dispersion law [3-7]. It is important that this nonlinearity results in the nonlinear focusing both in longitudinal and transverse directions and, thus, to the modulation instability (MI) of long input pulses and the wave collapse of short pulses [6,7]. The interaction of THz radiation with narrow-gap volume semiconductors like *n*-InSb and low dimensional structures like graphene is of great interest, because it gives a possibility to create both active and passive optical and electronic devices [6-10]. But when the compression of short envelope pulses occurs, the approximation of slowly varying amplitudes becomes doubtful, and the direct simulation of dynamic equations is needed.

In the report the nonlinear EM phenomena in the narrow-gap semiconductors like *n*-InSb are investigated by means of direct simulations of dynamic equations by the direct finite differences in time domain method. The nonlinearity of the electric current due to nonparabolicity of dispersion law of conduction electrons is considered as well as the dielectric nonlinearity. The electron concentrations are $n_0 = 10^{15} - 10^{16}$ cm^{-3}. Short input pulses are considered with the carrier frequency of THz range $\omega \geq 10^{13}$ s^{-1}. The carrier frequencies of the input pulses can be close to the frequency of the transverse optical phonons $\omega_T \sim 3\cdot10^{13} - 4.5\cdot10^{13}$ s^{-1}, and the nonlinear equation for the polarization should be included. The nonlinear phenomena are investigated that cause the nonlinear pulse compression. When the carrier frequency of the input EM pulse is chosen $\omega \leq 0.6\omega_T$, the signs of the cubic nonlinearity, dispersion and diffraction coefficients correspond to nonlinear focusing, or the compression of the pulse in all directions. At higher carrier frequencies $0.6\omega_T < \omega < 0.8\omega_T$ only the transverse compression occurs.

Model and basic formulas.

Consider volume *n*-InSb with the equilibrium electron concentration $n_0 \sim 10^{15}$ - 10^{16} cm^{-3} under the temperatures $T \geq 77$ K. The EM nonlinearity is due to the electron nonlinearity of the Kane dispersion law, or the nonstandard dependence of the electron energy E on the quasi-momentum $\boldsymbol{p}$ [3,4]. The hydrodynamic equation of motion of the electron gas can be presented as [4]:

$$\vec{v} = \frac{\partial \mathrm{E}}{\partial \vec{p}}; \quad \frac{d\vec{p}}{dt} = e\vec{E}; \quad \mathrm{E} = v_n(p^2 + \mathrm{p_g}^2)^{1/2}, \quad \mathrm{p_g} \equiv m^* v_n; \quad v_n \equiv \left(\frac{\mathrm{E}_g}{2m^*}\right)^{1/2} \qquad (1)$$

Here $\boldsymbol{v}$ is the electron velocity, m^* is the effective mass, E_g is the forbidden gap. Note that the dependence of the electron velocity on the electric field obtained from Eqs. (1) coincides with the expression derived from the kinetic theory [8]. The role of dissipation is discussed below.

The propagation of transversely polarized $E = E_x$ EM wave is investigated. The basic equations are the EM wave equation, the hydrodynamic equation for the electron velocity, and the equation for the lattice polarization $P/4\pi$:

$$\frac{\partial^2 E}{\partial z^2} - \Delta_\perp E - \frac{\varepsilon_\infty}{c^2}\frac{\partial^2 E}{\partial t^2} - \frac{1}{c^2}\frac{\partial^2 P}{\partial t^2} - \frac{4\pi e n_0}{c^2}\frac{\partial v}{\partial t} = 0;$$

$$\frac{\partial}{\partial t}\left\{\frac{v}{(1-\frac{v^2}{v_n^2})^{1/2}}\right\} + \nu v = \frac{e}{m^*}E; \qquad (2)$$

$$\frac{\partial^2 P}{\partial t^2} + \omega_T^2\left(1 + \frac{P^2}{P_0^2}\right)P + \gamma\frac{\partial P}{\partial t} = \omega_T^2(\varepsilon(0) - \varepsilon_\infty)E.$$

Here $\varepsilon(0)$, ε_∞ are low- and high-frequency dielectric permittivities, ω_T is the frequency of transverse optical phonons, γ is the lattice dissipation [4]. In the equation for the electron velocity the term with dissipation νv is included. Generally the collision frequency ν depends on the velocity. Also possible dielectric nonlinearity is included, the term with P^3 in the equation for the polarization. The parameter P_0 determines the value of this dielectric nonlinearity.

The new functions *u, A* are introduced:

$$\frac{v}{(1-\frac{v^2}{v_n^2})^{1/2}} \equiv u; \quad E \equiv \frac{\partial A}{\partial t}. \qquad (3)$$

Eqs. (2) can be rewritten as:

$$\Delta A - \frac{\varepsilon_\infty}{c^2}\frac{\partial^2 A}{\partial t^2} - \frac{1}{c^2}\frac{\partial P}{\partial t} - \frac{{\omega_p}^2 m^*}{ec^2}\frac{u}{(1+\frac{u^2}{{v_g}^2})^{1/2}} = 0;$$

$$\frac{\partial u}{\partial t} + \frac{\nu u}{(1+\frac{u^2}{{v_g}^2})^{1/2}} = \frac{e}{m^*}\frac{\partial A}{\partial t}; \qquad (4)$$

$$\frac{\partial^2 P}{\partial t^2} + {\omega_T}^2(1+\frac{P^2}{{P_0}^2})P + \gamma\frac{\partial P}{\partial t} = {\omega_T}^2(\varepsilon(0)-\varepsilon_\infty)\frac{\partial A}{\partial t}.$$

Here $\omega_p = (\frac{4\pi e^2 n_0}{m^*})^{1/2}$ is the electron plasma frequency.

In the linear case Eqs. (2) correspond to the following effective permittivity that includes both the polarization and the conductivity:

$$\varepsilon(\omega) = \varepsilon_\infty + \frac{{\omega_T}^2(\varepsilon(0)-\varepsilon_\infty)}{{\omega_T}^2 - \omega(\omega - i\gamma)} - \frac{{\omega_p}^2}{\omega(\omega - i\nu)}. \qquad (5)$$

One can see that the propagation of linear EM waves of THz range is possible for $\mathrm{Re}(\varepsilon(\omega)) > 0$, or within the frequency interval $\omega_p/\varepsilon(0)^{1/2} < \omega < \omega_T$.

To specify possible nonlinear effects for envelope pulses, write down a simple parabolic nonlinear equation for the slowly varying amplitude B:

$$\frac{\partial B}{\partial t} + v_g\frac{\partial B}{\partial z} + ig_1\frac{\partial^2 B}{\partial z^2} + ig_2\frac{\partial^2 B}{\partial y^2} + iN\,|B|^2 B + \Gamma B = 0;$$

$$v_g \equiv \frac{\partial\omega}{\partial k} > 0, \quad g_1 \equiv \frac{1}{2}\frac{\partial^2\omega}{\partial k^2}, \quad g_2 \equiv \frac{v_g}{2k} > 0; \quad A = \frac{1}{2}(B(z,y,t)e^{i(\omega t - kz)} + c.c.). \qquad (6)$$

Here v_g is the group velocity, g_1 is the dispersion coefficient, g_2 is the diffraction one, N is the coefficient of the cubic nonlinearity; Γ is the wave dissipation. The carrier frequency ω and the wave number k are connected by the linear dispersion equation $k - (\omega/c)\,(\varepsilon(\omega))^{1/2} = 0$. The nonlinear propagation of envelope pulses depends on the signs of the products $g_1 N$ and $g_2 N$ [11].

In Fig. 1 the dependencies are given of the real part of the wave number $k'(\omega)$, the imaginary part $k''(\omega)$, the group velocity $v_g(\omega)$, the dispersion coefficient $g_1(\omega)$, and the diffraction coefficient $g_2(\omega)$ on the frequency ω. The parameters of n-InSb are: the electron effective mass is $m^* = 0.014m_e$, the frequency of transverse optical phonons is $\omega_T = 3.376\cdot10^{13}$ s^{-1}, the electron concentration is $n_0 = 10^{16}$ cm^{-3}, low and high-frequency permittivities are $\varepsilon(0) = 17.1$, $\varepsilon_\infty = 15.2$; the lattice dissipation is $\gamma = 2\cdot10^{11}$ s^{-1}, the electron collision frequency is $\nu = 5\cdot10^{11}$ s^{-1}.

One can see that the dispersion coefficient g_1 changes its sign at $\omega \approx 0.6\omega_T$. When the nonlinearity is determined by the nonparabolicity of the electron dispersion (1), the sign of the nonlinearity is $N > 0$ [6,7]. Because the diffraction coefficient is $g_2 > 0$, in the frequency interval $\omega_p/\varepsilon(0)^{1/2} < \omega < 0.6\omega_T$ the nonlinear

focusing, both longitudinal and transverse, occurs: $g_{1,2}N > 0$. Thus, the volume nonlinearity of *n*-InSb results in the compression of the pulses in all directions in the pointed above frequency interval.

At higher frequencies only the transverse compression occurs. But, when the doping level is small, the nonlinearity is purely dielectric, and its sign is $N < 0$. Therefore the longitudinal compression of envelope pulses occurs there in the *i*-InSb. But the dielectric nonlinearity is semiconductors is usually smaller than one connected with the electron gas.

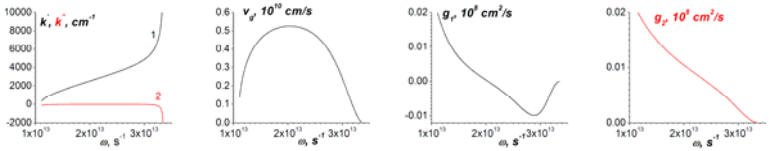

a) b) c) d)

Fig. 1. Part a) is the linear dispersion relation $k'(\omega)$, curve 1, and the imaginary part $k''(\omega)$, curve 2; part b) is the group velocity $v_g\omega)$; part c) is the dispersion coefficient $g_1(\omega)$; part d) is the diffraction one $g_2(\omega)$ for the electron concentration in *n*-InSb $n_0 = 10^{16}$ cm^{-3} and the collision frequency $\nu = 5\cdot10^{11}$ s^{-1}.

Note that also there is a possibility to realize the resonant interaction between the first ω_1 and the third $\omega_3 = 3\omega_1$ harmonics of THz EM waves: $k(\omega_3) \approx 3k(\omega_1)$, when the first harmonic is chosen $\omega_1 \approx 1\cdot10^{13}$ s^{-1}, see Fig.1, a. But this frequency tripling needs a special consideration.

Simulations.

The main goal of the simulations is to investigate the nonlinear compression of input envelope pulses, which include several oscillation periods. The case of axially symmetric input pulses is considered; the input pulse is:

$$E = E_0 \cos(\omega(t-t_1))\exp(-(\frac{t-t_1}{t_0})^8)\exp(-(\frac{\rho}{\rho_0})^8)\,. \qquad (7)$$

The shape of the envelope of the input pulse is almost rectangular both for time t and for the transverse radial coordinate ρ. The parameters of volume *n*-InSb are: the electron concentration is $n_0 = 10^{16}$ cm^{-3}, electron collision frequency is $\nu = 5\cdot10^{11}$ s^{-1}, $\omega_T = 3.376\cdot10^{13}$ s^{-1}. The carrier frequency ω has been chosen 10^{13} s$^{-1} < \omega < 2\cdot10^{13}$ s$^{-1} \equiv 0.6\omega_T$.

The direct simulations of Eqs. (4) have been done. The explicit difference schemes have been used; the temporal step is chosen from the condition of numerical stability.

The results of the simulations are given in Figs. 2-5. The electric field is normalized to $E_n = m^*v_0/(et_n) \approx 2$ abs. units ≈ 0.6 kV/cm, where $t_n = 10^{-12}$ s $\equiv 1$ ps. In all Figs. the maximum values of the THz electric field are depicted, as well as spatial distributions of the electric field within *n*-InSb. The center of the input pulse is at $t_1 = 3$ ps.

In Figs. 2-4 there are the dynamics of short envelope pulses at the carrier frequency $\omega = 1.4 \cdot 10^{13}$ s^{-1}. It is seen that in the linear case, Fig. 2, both wave dispersion and diffraction cause the broadening of the pulse. But when the input amplitude is higher and corresponds to small nonlinearity, Fig. 3, some pulse compression occurs. When the input amplitude becomes higher, Fig. 4, essential compression both in the longitudinal and transverse directions occurs. The transverse width ρ_0 of the input pulse is optimal for compression at this carrier frequency, compare Fig.4, c) and d).

In Fig. 5 the simulations of pulse propagation are given at higher carrier frequency $\omega = 1.6 \cdot 10^{13}$ s^{-1}. It is seen that the bigger transverse compression occurs there, whereas the longitudinal compression is smaller, compared with Fig. 4.

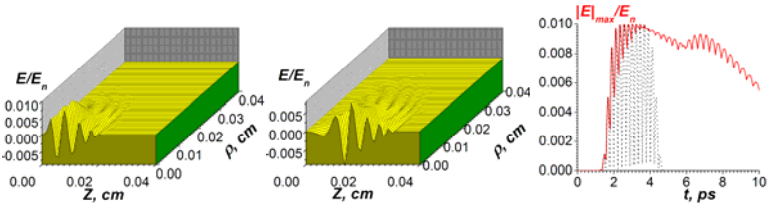

a) b) c)

Fig. 2. The linear propagation of the THz pulse of a small input amplitude E_{i0} =6 V/cm. The carrier frequency is $\omega = 1.4 \cdot 10^{13}$ s^{-1}. The transverse width of the incident pulse is ρ_0 = 0.01 cm, the duration is t_0 = 1.4 ps. Part a) is the spatial distribution $E(z, \rho)$ at t = 5ps; part b) is $E(z, \rho)$ at t = 7 ps. Part c) is the maximum value of $|E(z, \rho)|$ under different moments of time, solid line; the dependence of $|E(z=0, \rho=0,t)|$ is given by the dot line.

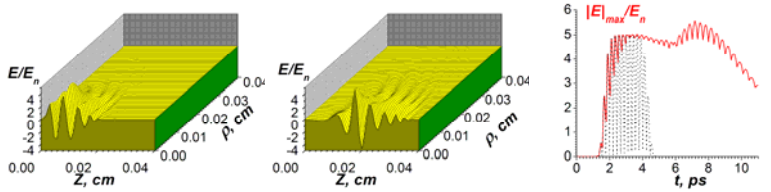

a) b) c)

Fig. 3. The nonlinear propagation of the THz pulse of a finite input amplitude E_{i0} =3 kV/cm. $\omega = 1.4 \cdot 10^{13}$ s^{-1}, ρ_0 = 0.01 cm, t_0 = 1.4 ps. Part a) is the spatial distribution $E(z, \rho)$ at t = 5 ps; part b) is $E(z, \rho)$ at t = 8 ps. Part c) is the maximum value of $|E(z, \rho)|$ under different moments of time, solid line; the dependence of $|E(z=0, \rho=0,t)|$ is given by the dot line.

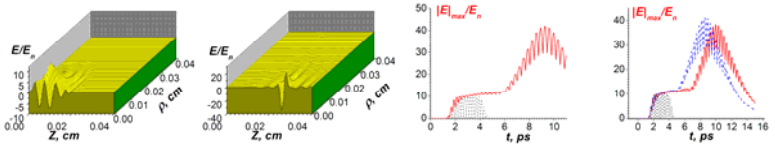

a) b) c) d)

Fig. 4. The nonlinear propagation of the THz pulse of a finite input amplitude E_{i0} =6 kV/cm. $\omega = 1.4 \cdot 10^{13}$ s^{-1}, $\rho_0 = 0.01$ cm, $t_0 = 1.4$ ps. Part a) is the spatial distribution $E(z, \rho)$ at $t =$ 5 ps; part b) is $E(z, \rho)$ at $t = 9.5$ ps. Part c) is the maximum value of $|E(z, \rho)|$ under different moments of time, solid line; the dependence of $|E(z=0, \rho=0,t)|$ is given by the dot line. Part d) is the maximum values of $|E(z, \rho)|$ for another values of input transverse widths $\rho_0 = 0.009$ cm, dash curve, and $\rho_0 = 0.011$ cm, solid curve.

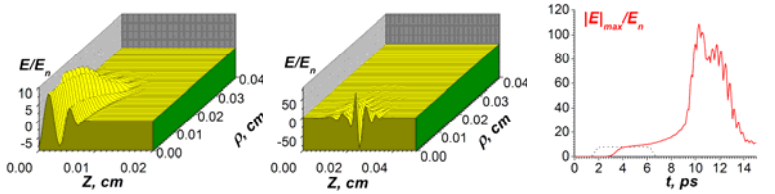

a) b) c)

Fig. 5. The nonlinear propagation of the THz pulse of a finite input amplitude E_{i0} =4.8 kV/cm. $\omega = 1.6 \cdot 10^{13}$ s^{-1}, $\rho_0 = 0.025$ cm, $t_0 = 1.4$ ps. Part a) is the spatial distribution $E(z, \rho)$ at $t =$ 5 ps; part b) is $E(z, \rho)$ at $t = 10$ ps. Part c) is the maximum value of $|E(z, \rho)|$ under different moments of time, solid line; the dependence of $|E(z=0, \rho=0,t)|$ is given by the dot line.

Analogous pulse compression takes place in *n*-InAs, where the electron effective mass $m^* = 0.023 m_e$ is bigger than in *n*-InSb. But the frequency of optical phonons is also bigger, $\omega_T = 4.046 \cdot 10^{13}$ s^{-1}. Therefore the frequency range for observation of the pointed above effects may be wider than in *n*-InSb.

When the electron collision frequency increases with the increase of the velocity, the pulse compression is also possible, but maximum values of THz electric field decrease.

Therefore, the nonlinear compression of THz pulses is possible in volume *n*-InSb in the specified frequency range defined by the plasma frequency and the frequency of the transverse optical phonons.

Conclusions.

The nonlinear longitudinal and transverse compression of short envelope terahertz pulses can be realized in narrow-gap semiconductors like *n*-InSb, *n*-InAs. The nonlinearity is due to the nonparabolicity of the dependence of the electron energy on the quasi-momentum. The carrier frequency should be chosen above the

cut-off frequency and below the frequency of transverse optical phonons and is of about 1.5 THz < f < 3.2 THz for the propagation in n-InSb.

The finite differences in time domain simulations of dynamic equations have been used. In the specified frequency interval the nonlinear pulse compression results in the powerful terahertz pulses with the transverse localization < 0.01 cm and durations 1 – 3 ps.

References

1. Siegel P.H. Terahertz Technology. IEEE Trans. MTT.–2002. – Vol. 50. - P.910-919.
2. Perenzoni M. and Paul D.J. (Eds.). Physics and Applications of Terahertz Radiation. Springer. –New York, 2014. - 255 p.
3. Bass F.G. and Bulgakov A.A. Kinetic and Electrodynamic Phenomena in Classical and Quantum Semiconductor Superlattices. Nova Publ. –New York, 1997. - 501 p. (The Russian version: Nauka. – Moscow, 1989).
4. Yu P.Y. and Cardona M. Fundamentals of Semiconductors. Physics and Materials Properties. Springer. -New York, 2010. -775 p.
5. Levinshtein M., Rumyantsev S., and Shur M. Handbook Series on Semiconductor Parameters. Vol. 1. World Scientific - Singapore, 1999. - 280 p.
6. Rapoport Yu. G., Grimalsky V.V., Castrejon-M. C., Koshevaya S.V., Kivshar Yu.S. Nonlinear Spatiotemporal Focusing of Terahertz Pulses in the Structures with Graphene Layers. Proc. 2014 IEEE 34th International Scientific Conference on Electronics and Nanotechnology, ELNANO 2014. - P. 31-34, Kyiv; Ukraine; 15-18 April 2014.
7. Rapoport Yu. G., Grimalsky V.V., Castrejon-M. C., Koshevaya S.V. Modulation Instability of Terahertz Pulses in the Structures with n-InSb Layers. Proc. 2014 IEEE 35th International Scientific Conference on Electronics and Nanotechnology, ELNANO 2015. - P. 124-127, Kyiv; Ukraine; 19-21 April 2015.
8. Grimalsky V.V., Castrejon-M. C., Koshevaya S.V., Rapoport Yu. G. Nonlinear Properties of Electron Gas in n-InSb and Graphene in THz Range Under Finite Temperatures. Proc. 2017 IEEE 37th International Scientific Conference on Electronics and Nanotechnology, ELNANO 2017. - P. 37-41, Kyiv; Ukraine; 18-20 April 2017.
9. Mikhailov S.A. Electromagnetic Response of Electrons in Graphene: Non-Linear Effects. Physica E, 2008 - Vol. 40. - P. 2626–2629.
10. Dong H., Conti C., and Biancalana F. Terahertz Relativistic Spatial Solitons in Doped Graphene Metamaterials. 2011. - arXiv:1107.5803 [physics.optics].
11. Kivshar Y.S. and Agrawal G.P. Optical Solitons. From Fibers to Photonic Crystals. Academic Press. –New York, 2003. - 540 p.